

# Implementation and application of the actuator line model by OpenFOAM for a vertical axis wind turbine

L Riva<sup>1\*</sup>, K-E Giljarhus<sup>2</sup>, B Hjertager<sup>2</sup> and S M Kalvig<sup>2</sup>

<sup>1</sup>Department of Engineering Sciences, University of Agder, Norway

<sup>2</sup>Department of Mechanical and Structural Engineering and Material Science, University of Stavanger, Norway

\*Contact author: lorenzor@uia.no

**Abstract.** University of Stavanger has started The Smart Sustainable Campus & Energy Lab project, to gain knowledge and facilitate project based education in the field of renewable and sustainable energy and increase the research effort in the same area. This project includes the future installation of a vertical axis wind turbine on the campus roof. A newly developed Computational Fluid Dynamics (CFD) model by OpenFOAM have been implemented to study the wind behavior over the building and the turbine performance. The online available wind turbine model case from Bachant, Goude and Wosnik from 2016 is used as the starting point. This is a Reynolds-Averaged Navier-Stokes equations (RANS) case set up that uses the Actuator Line Model. The available test case considers a water tank with controlled external parameters. Bachant et al.'s model has been modified to study a VAWT in the atmospheric boundary layer. Various simulations have been performed trying to verify the models use and suitability. Simulation outcomes help to understand the impact of the surroundings on the turbine as well as its reaction to parameters changes. The developed model can be used for wind energy and flow simulations for both onshore and offshore applications.

## 1. Introduction

Oil export has long been a significant source of income in Norway. The recent drops in the oil price and a considerable export reduction have forced Norway to start questioning about the solidity of its economic structure: it must be updated according to the new political and economic scenario. New-Renewable energies and technology (hydropower not included) have been targeted as one of the possible new economic hubs. In 2014, investment to sustainable energies passed from circa 2-3 billion Euros to 4-5 billion Euros [1].

Aside economic reason, there are also environmental concerns. In December 2015, Norway signed the COP21 agreement. It pledged to reach carbon neutrality by 2030 and to bring greenhouse emissions 40% below the 1990 values [2]. Norway has hence joined European Union (EU) funding projects to foster such transition.

Wind energy is allegedly one of the most promising renewable sources. It has grown dramatically for the last decades. Focusing on EU, if in 2000 electricity production share from wind energy was below 1.5%, in 2014 reached the 14.1% and is forecasted to achieve the 23% by 2030 [3]. An even more dramatic growth has found place in Norway: between 2015 and 2016 the wind power production for year passed from 2.5 TWh to 10 TWh [4]. This transition is related to the will of the principal



national companies to open new ways of investment. The intention is to transfer the knowledge of offshore technologies accrued through decades of oil and gas research and development to this sector; trying to keep up with the international market. The Norwegian Wind Energy Association (NORWEA) esteemed investments in Norway on wind energy in 2015 were above 2.4 billion dollars [4]. University of Stavanger has started The Smart Sustainable Campus & Energy Lab project, to gain knowledge and facilitate project based education in the field of renewable and sustainable energy and increase the research effort in the same area. The project envisages the installation of a set of built environment wind turbines (BEWT), instrumented with measurement devices. Ivar Langen's (IL) building, which is indicated in Figure 1, has been identified as possible target point to install one or more turbines. This building represents a good tradeoff between visibility and efficiency.

A flexible CFD set up for future detailed wind flow analysis and wind turbine power performance simulations for the campus was suggested. This need was addressed in Lorenzo Riva's Master Thesis (2016) and this paper is based on Riva's thesis [5]. The Actuator Line Model (ALM) is used for wind turbine representation. This model represents a good trade-off between accuracy and time consumption. Originally developed by Sørensen and Shen [6] for HAWT in 2002, it has been recently updated for VAWT by Shamsoddin and Porté-Angel [7] and by Schito, Bernini and Zasso [8].



**Figure 1.** UiS Campus and IL building (UiS courtesy)

Bachant et al. [9] released an open-source case based on OpenFOAM [10] with the library necessary to run the case [11]. This model has been selected for this case. Unlike the laboratory experiments with controlled parameters, in the present study the wind flow is simulated according to the atmospheric conditions. No literature has been found documenting ALM outdoor use for VAWT. This is also a big challenge since there are no studies to compare the model implemented with. This model may furnish an example of ambient-condition case, useful for analyses of different contexts and landscapes. Application for onshore as well as offshore surroundings might be considered. In a recent master thesis project, 'Wind Flow Simulation over Fish Farm Feed Barge' by Svein Erik Nuland [12], the same model has been applied for offshore analyses. The work of Nuland demonstrated the feasibility and elasticity of the model.

## 2. Theory

### 2.1. Atmospheric boundary layer (ABL)

The behavior of the moving fluid is described by Navier-Stokes equations. In the current study, Reynolds-Averaged Navier-Stokes equations (RANS) with the  $k-\epsilon$  model has been adopted. This decision comes from the necessity to find a good compromise between the computational cost and the accuracy of the results. In particular, the RANS constants have been modified to fit better the atmospheric conditions.

There are several challenges related to the CFD modelling of the atmospheric boundary layer, for example, it changes along the flow direction and that makes the flow not homogeneous. As observed by

[13], the  $k$ - $\varepsilon$  model and the boundary layer need to be modified to account for the wind behavior in atmospheric condition with a greater degree of accuracy. Among several possible solutions, Hargreaves and Wright considerations have become very popular because it is easily applicable [14]. As previously stated, the lowest part of atmosphere is involved. It must be therefore modelled. The horizontally homogeneous turbulent surface layer (HHTSL) suits it well.

This approach relies on the following assumptions:

- 1 – the vertical velocity is zero;
- 2 – the pressure is constant in both the vertical and stream-wise directions;
- 3 – the shear stress is constant throughout the boundary layer;
- 4 – flow is steady state.

These assumptions lead to:

$$u = \frac{u_\tau}{k} \ln\left(\frac{z + z_0}{z_0}\right) \quad (1)$$

$$k = \frac{u_\tau^2}{\sqrt{C_\tau}} \quad (2)$$

$$\varepsilon = \frac{u_\tau^3}{\kappa(z + z_0)} \quad (3)$$

With  $u$  as flow velocity  $z_0$  as roughness length and  $z$  as height.  $C_\tau$  and  $\kappa$  (Von Karman constant) are constrains. Friction velocity  $u_\tau$  is:

$$u_\tau = \sqrt{\frac{\tau}{\rho}} \quad (4)$$

where  $\rho$  is the density. OpenFOAM permits to include directly the ABL conditions. A rough wall function is also used at the ground.

## 2.2. Actuator line model (ALM)

The ALM is based on the classical blade element theory combined with a Navier- Stokes description of the flow field. It treats turbine blade as actuator line elements, defined by their quarter-chord location, and for which 2-D profile lift and drag coefficients are known [9]. A diagram is shown in Figure 2, where  $U_{in}$  is the local inflow wind velocity,  $U_{rel}$  is the relative velocity,  $-\omega r$  is the apparent wind velocity due to tangential blade speed,  $M$  is the pitching moment,  $\theta$  is the rotational angle of attack (positive counterclockwise),  $r$  is the radius,  $\alpha$  is the angle of attack,  $F_l$  is the lift force,  $F_d$  is the drag force.

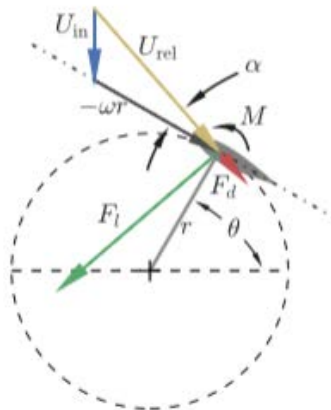


**Figure 2.** Visualization of the ALM by vector diagram [8]

Once the drag and the lift coefficients are provided by tables, it is possible to compute the lift force, the drag force and the pitching moment. Forces are then projected onto the rotor coordinate system to calculate torque, overall drag and other quantities. The same method is adopted for the turbine shaft and the blade support struts. Finally, the force on the actuator line is added to the Navier-Stokes equations.

For small turbines, the solidity is usually small and the tip speed ratio (TSR), which is the ratio between the relative velocity at the tip of the blade and the free stream velocity, is low. That is the case for instance of the turbine involved here. Unsteadiness will hence be significant and needs to be considered. This will affect mainly angle of attack and relative velocity. In [9], the issue is addressed including dynamic stall implementation and other corrections.

Dynamic stall is computed by a model developed by Sheng et al. [15]. It is derived from the Leishman-Beddoes semi-empirical model. Among the dynamic stall models, this is one of the most popular, probably due to its physical representation of the overall unsteady aerodynamic problem. Basically, it models the dynamic stall introducing a boundary layer delay method and a strategy to take into consideration the dynamic vortex [9]. Sheng et al. have tailored the original model for low Mach numbers. The model is included into the library turbinesFoam [11], which the ALM calls during its application. Inside the ALM, angle of attack is sampled from the flow field. Lift and drag coefficients are then corrected considering the effects due to accelerating the fluid [9].

This model provides also corrections due to the so-called curvature effects, which are caused by the rotation and bring to a variable chord-wise angle of attack distribution; and due to the end effects [9]: vortex lines may not end in a fluid, but must either form closed loops or extend to boundaries. As consequence lift distribution may be affected.

### **3. Modeling approach**

In the following section, a brief description of the model is given. The input values, critical steps and the main assumptions that have been considered and processed during the implementation.

#### *3.1. Turbine description*

Since the UiS project has not yet selected any turbine, it has been decided as a preliminary step to choose directly the turbine used into the open-source case [10]. The turbine is named UNH-RVAT (University of the New Hampshire –Reference Vertical Axis Turbine). Design is performed with the aim of furnishing a reference layout for VAWT and can be seen in Figure 3. The UNH-RVAT turbine has three blades made of NACA 0020 profiles with a 0.14 m chord. The blades are mounted at mid-chord with respect to the turbine axis, and the turbine has a height of 1 m and a diameter of 1 m [16].

#### *3.2. Airfoil dataset*

Following reference case suggestions, the airfoil profile NACA 0021 has been used, with dataset taken from [17]. This database has some limitations regarding the numerical extrapolations of data from other measurements. Nevertheless, this dataset is likely the most comprehensive available with respect to variety of profiles and ranges of Reynolds numbers [9]. The complete NACA 0020 dataset is not available. However, according to [9], the small difference in foil thickness is assumed to be negligible.

#### *3.3. Campus model*

At the beginning of the current study, no existing detailed three-dimensional models of the campus were available. It has been necessary to design a new one. By the utility snappyHexMesh, which is a mesh generation utility, it is possible to generate a three-dimensional mesh from tri-surfaces in STL format. Hence, first a 3D STL file of the campus is necessary. The file has been generated by the collaboration with Ibrahim Mufti Pradityo, an Urban Planning and Design student at UiS. Due to environmental constrains, the expected main wind directions are from South and West. The eastern part of the campus, considered not influential for the observed case, has been neglected. Ivar Langen building, which is the target building, and Kjølvs Egeland building, which is the one beside it, have been

modelled starting from the basic drawings UiS provided. For the other buildings, no 2D models were available. They were made based of images obtained on Google Maps. Terrain has been reconstructed importing a set of SOSI-points. SOSI (Systematic Organization of Spatial Information) is a geospatial vector data format used in Norway. The overall 3D model was then implemented on Revit 2017, a building information modelling (BIM) software developed by Autodesk. Revit 2017 cannot export STL file. The 3D model has been hence imported into Sketchup, a 3D modelling software. Here it has been located on suitable coordinates in the X-Y-Z system and finally exported as STL file. Coordinates have been selected so that the positive verse of the axis-x coincides with east and the positive verse of the axis-y with north. Figure 4 shows the final design of the campus.



**Figure 3.** UNH-RVAT turbine [16]

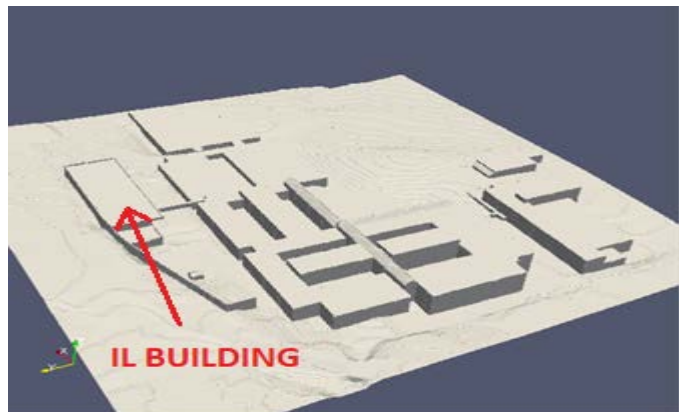


**Figure 4.** STL 3D Campus Model

### 3.4. Computational mesh

The computational domain is 300 m x 300 m x 100 m. It is initially divided in 72000 cells of 5 m x 5 m x 5 m. This size has been selected based on tests carried out as preliminary step, where several cells dimension have been proposed, in order to obtain reasonable time of simulation and accuracy [5]. The grid must be refined to resolve the details in the campus models and for the turbine representation. The location of the turbine has been chosen according to preliminary wind simulations over the campus. The center of the turbine is situated in  $x = 190$  m,  $y = 240$  m,  $z = 25$  m (building height is approximately 23.5 m). The turbine is 45 m far from the west-face of the building, 40 m from the east-face, 10 m from the south-face and 15 m from the north-face. Figure 5 displays the selected location, at the final step of simulation, with different streamlines and sights. Streamlines dimension has been accentuated to ease the visibility and color indicates the velocity, which is named *UMagnitude* and measured in m/s. Campus and ground are colored showing the relative pressure normalized with the density (with zero set at atmospheric pressure). The wind has been simulated in the preliminary study with the inlet value of 15 m/s, in order to provide same Reynolds number of [9]. It has been simulated blowing from west and is strongly affected by the fence located 85 m before the IL building.

Despite the fence is actually not very tall, it is located almost at the same height of the roof. Turbulence is generated, slowing the flow. Wind streamlines look more uniform in the part of the roof where the turbine is located. Wind flow is expected to have therefore less velocity losses and to maintain its velocity profile close to the undisturbed field. The turbine should hence manifest higher performance than if set on other locations over the building. The turbine is inserted into a sequence of four refinement boxes. The outer box is made of 1.25 m cube cells, medium-outer box of 0.3125 m cube cells, medium-inner box of 0.078 m cube cells and inner box of 0.039 m cube cells. The choice of the number of layers and their values comes from the necessity to guarantee a soft transition between the external grid cell dimension and the one characterizing the turbine. A rapid and rough change might bring to errors in the meshing process and in discontinuities in solving, so the collapse of the

simulation. A slow and meticulous change instead might slow down the simulation significantly. Turbine is made of 0.039 m cube cells. Overall result after the meshing process is shown in Figure 6. The total number of cells are approximately 1 million.

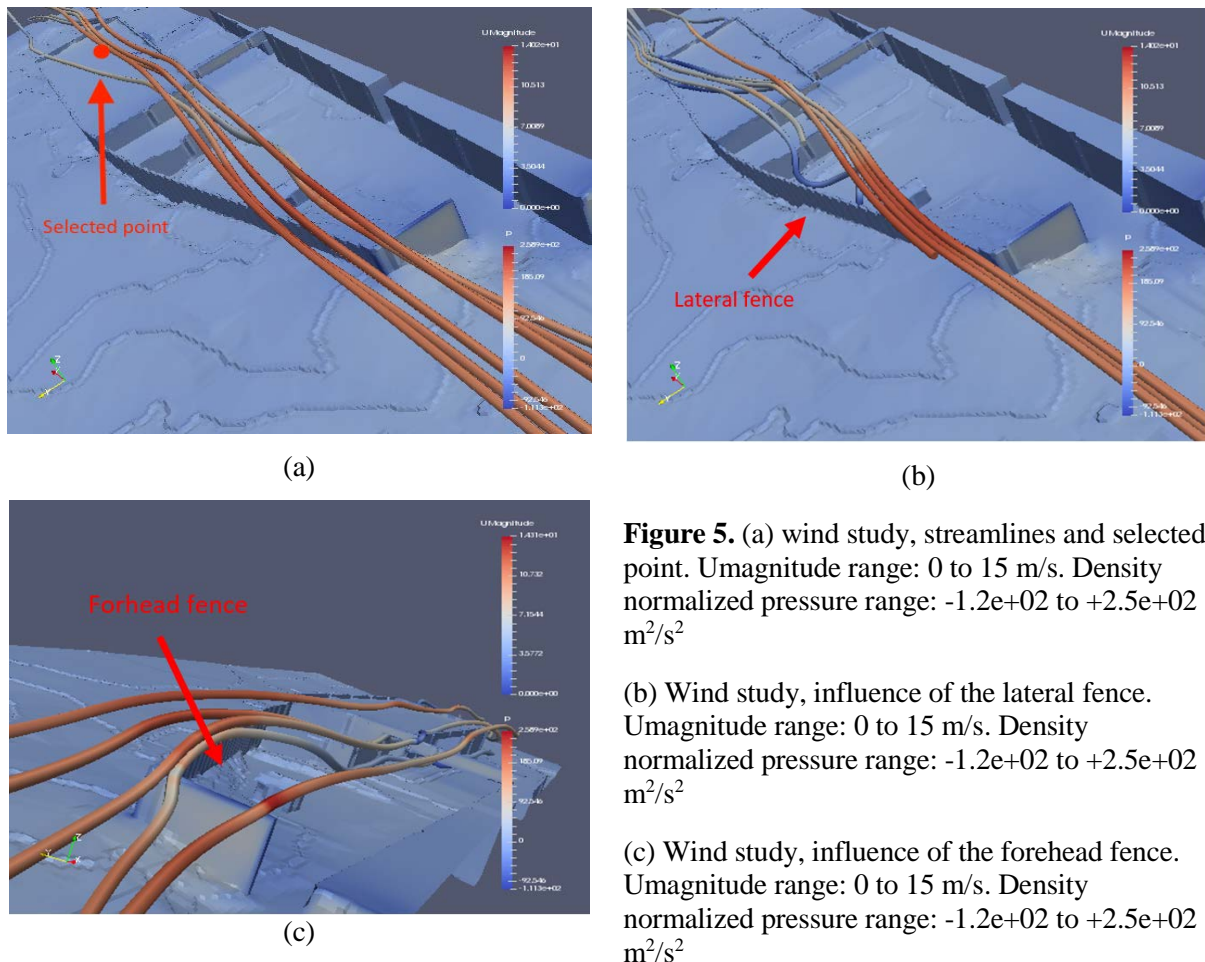


**Figure 5.** (a) wind study, streamlines and selected point. Umagnitude range: 0 to 15 m/s. Density normalized pressure range: -1.2e+02 to +2.5e+02 m<sup>2</sup>/s<sup>2</sup>

(b) Wind study, influence of the lateral fence. Umagnitude range: 0 to 15 m/s. Density normalized pressure range: -1.2e+02 to +2.5e+02 m<sup>2</sup>/s<sup>2</sup>

(c) Wind study, influence of the forehead fence. Umagnitude range: 0 to 15 m/s. Density normalized pressure range: -1.2e+02 to +2.5e+02 m<sup>2</sup>/s<sup>2</sup>

### 3.5. Numerical settings

The case is implemented on OpenFOAM 3. Bachant's case has been modified and adapted. First modification was to adapt the case to air. This can be done through the transportProperties dictionary inside the constant folder. The transportModel selected is Newtonian, and nu is 1.5e-05. Turbulence model is k-ε and coefficients follows [14]. The reference velocity for the ABL is set to 10 m/s, reference height set to 25 m and roughness set to 0.01 m. Following [14], initial values are 1.3 m<sup>2</sup>/s<sup>2</sup> for k and 0.01 m<sup>2</sup>/s<sup>3</sup> for ε. The time scheme selected is backward, which has second-order accuracy. For the divergence schemes, second-order linear upwind schemes are selected. Pressure solvers are GAMG type.

The principle of this solver is to generate a quick solution on a small number cells mesh, to map then this solution onto a finer mesh and to use it as an initial guess to obtain an accurate solution on the fine mesh [18]. With respect to other common solvers it is faster. In this case it has been also smoothed with a DICGaussSeidel (diagonal incomplete-Cholesky/LU with Gauss-Seidel) smoother. Other parameters are treated with a smoothSolver and as smoother the symGaussSeidel (symmetric Gauss-Seidel) has been used. Besides, nOuterCorrectors enables looping over the entire system of equations within a time step, representing the total number of times the system is solved [18]. If, as in this case, it is 1, solver is

replicating PISO algorithm. NCorrectors does the same with only pressure and momentum equations and it is 2.

Time settings require the selection of the overall time of simulation and the duration of each time step. This choice must consider the complex geometry and physics of the case: a turbine is spinning, affected by an evolving flow surrounding. Settings must therefore be chosen in order to ensure that the rotation of the turbine is adequately simulated. The time step is chosen according to the rotational speed of the turbine. Keeping  $TSR = 1.9$  (which is the optimal value in [9]) and  $v_{wind} = 10$  m/s, it will be  $\omega = 38$  rad/s. It means turbine takes 0.165 s to complete a rotation. A time step of 0.001 s has been chosen. There are 165 steps per revolution and, according to the reference article [9], this is sufficient to guarantee accuracy.

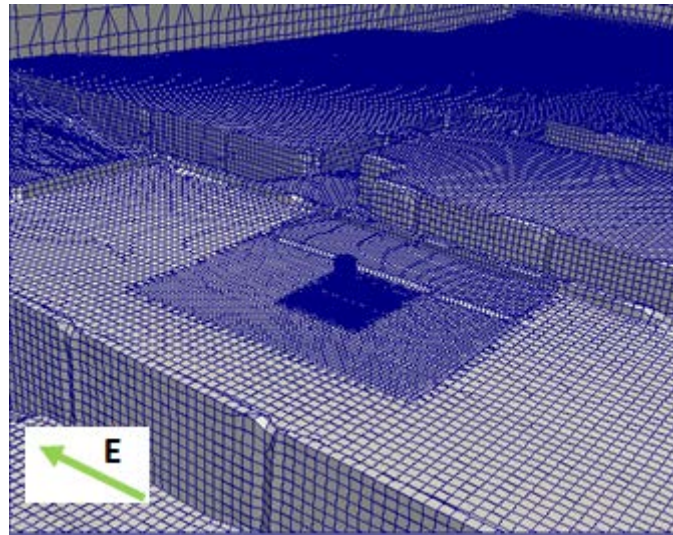


**Figure 6.** Final mesh and eastward direction.

The total simulation time is chosen based on the time it takes for the overall flow field to reach a stable solution, that is when the wind velocity profile is uniform throughout the mesh. By several simulations runs, it was found that a simulation time of 30 s guarantees good stability and homogeneity throughout the mesh. This value is a compromise between the necessity of guaranteeing acceptable simulation time and a good accuracy. Higher time would be more appropriated to provide precise outputs. Turbine is defined by fvOptions, which calls the turbinesFoam library, selects the model and lets the user activate and change some model parameters. It is important to remind that, according to fvOptions selections, the drag and the lift coefficient will be modified into the turbinesFoam library, before being used. These forces will be used both to solve the discretized Navier-Stokes equations and to compute the torque on the turbine. Torque is then directly used into the library to obtain the torque coefficient by:

$$C_{torque} = \frac{M}{0.5 A_{frontal} v_{freeStream}^2 R} \quad (5)$$

as well as the power coefficient:

$$C_{power} = C_{torque} TSR \quad (6)$$

where  $A_{frontal}$  is the frontal area,  $v_{freeStream}$  is the free stream velocity,  $R$  is the radius and  $TSR$  is the Tip Speed Ratio. As evident the torque coefficient uses the free stream velocity. Power coefficient hence refers to this parameter. This decision can fit well a lab surrounding where flow can be easily controlled. In an open air surrounding, velocity changes significantly. Power coefficient might be very

different from the value the turbine is actually experiencing. One could state that the surrounding itself is part of the turbine performance and accept to keep this value. Here it has been decided to focus on the performance of the turbine, regardless the surrounding. It has been decided to correct the power coefficient using the average value, of the last 3 s, of the sampled velocities along the z-axis of the turbine (from  $z = 24.5$  to  $z = 25.5$ ). Turbine obviously affects the surrounding; therefore, this sampling must be done somewhere upstream the turbine location in order to catch the real wind speed that might be exploited. Sampling has been done in  $x/R = -10$ . This distance has been selected since it is enough far not to be influenced by the turbine behavior. The power coefficient then becomes:

$$C_{power,new} = C_{power} \frac{v_{freeStream}^2}{v_{sampled}^2} \quad (7)$$

where  $v_{sampled}$  is the sampled average velocity.

### 3.6. Wind data set collection

During the realization of this study, a set of wind data recorded from 2003 to 2013 has been found. The anemometer is located in the eastern side of the adjacent building. The wind monitoring was developed and measurement data acquired by a former staff at the department at the University of Stavanger. It has been considered useful to analyze the data to possibly enrich the insight of the problem. A wind rose has been therefore drawn from these data and is shown in Figure 7. The dominant wind direction is from south. West and east share a considerable part. North has been neglected because of physical obstacles (part of the building and environment). According to the wind rose, a 10-min mean wind speed range between 4 m/s and 6 m/s is very common. However higher speeds have been recorded, up to 12 m/s.

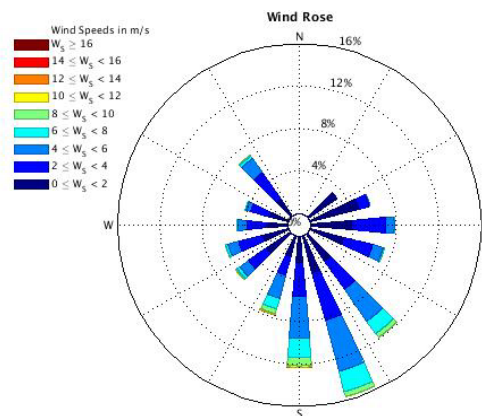


Figure 7. Wind rose

## 4. Results

This work aims to be the first stone of a path that will be improved and better shaped over the time. Many studies can be still carried out to guarantee a better model. Moreover, as the turbines will be mounted, the computational part will be enriched by the experimental outputs. Therefore, in the meantime, model has been tested by some sensitivity analyses; trying to understand how it would react. Then model has been tested changing the TSR and wind velocity. The performance has been compared installing the turbine in different reasonable locations.

### 4.1. Model analysis

The case studied has a wind speed at the inlet of 10 m/s at the turbine height (25 m). TSR is 1.9, which was the optimal value in the reference paper. Values are extrapolated as average of the last 3 s of

simulation. The velocity field inside the turbine area is characterized by a central low-speed zone, which is typical of VAWT aerodynamics. The velocity profile along the x-axis,  $U_{wind}$ , is shown in Figure 8. Compared to the results in e.g. [6] and [7], the profile here does not show an almost symmetric trend. This condition is due to the difference in value of the wind speed along the y-axis. As Figure 8 shows, 1.5 m before hitting the turbine entrance area, wind is less than 10 m/s in  $y/R = -3$  and below 9 m/s in  $y/R = 3$ . Figure 8 shows that the turbine affects wind field even after a relatively long distance: wake is still strong after 1.5 m and evident after 3 m. Figure 9 shows the turbulent kinetic energy along the x-axis. The plot shows that the turbulent kinetic energy follows the expected trend, which for example can be compared to [9] and [19]. As for velocity, also this parameter presents different values on each side of the y-axis. The wake is visible in the plot in terms of an increased kinetic energy. Looking at Figure 9, it seems that the model has failed to catch the usual drop at the center of the turbine. This lack might be related either to an insufficient number of cells along the y-axis. Nevertheless, the curve at  $x/R = 0$  is characterized by two small peaks that might hide the drop in the middle.

Figure 10 shows forces (per unit density, assuming incompressible flow) in central part of the turbine. Figure 10a visualizes the distribution of the forces around the actuator line at half height of the turbine, Figure 10b visualizes it at the center part of the turbine. Forces along the actuator line are computed by the Actuator Line Model and then projected onto the flow field as a source term in the momentum equation. Following [9], the source term is tapered from its maximum value away from the actuator line by means of a spherical Gaussian factor, to avoid instability due to steep gradients. Figure suggests that forces get their maximum value around the windward part of the rotation (rotation in the counter clockwise direction). This phenomenon is a typical aerodynamics feature in VAWT.

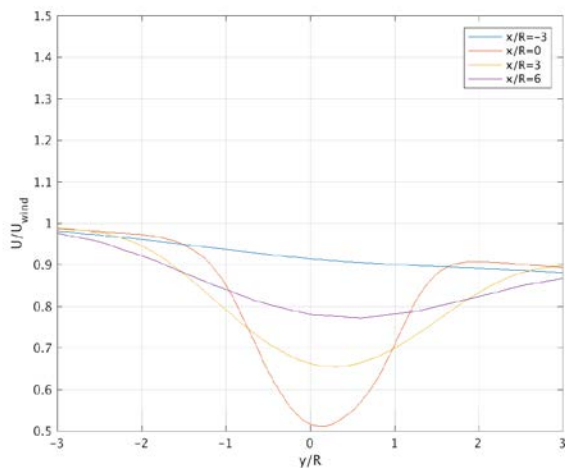


**Figure 8.** Velocity profile along the x-axis

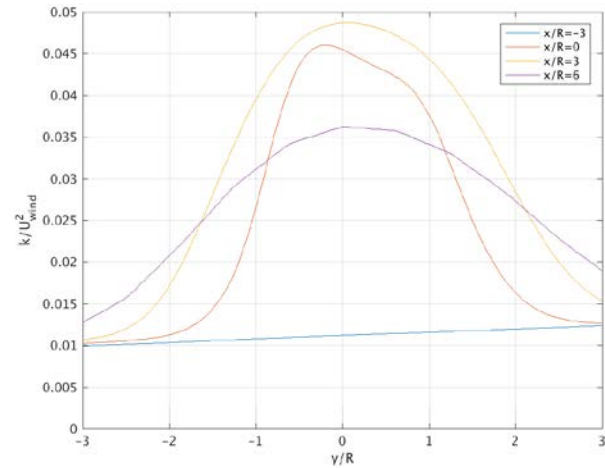


**Figure 9.** Turbulent kinetic energy profile along the x-axis

#### 4.2. TSR optimization

The first parameter studied is the TSR. Turbine has been tested with six values: 0.9, 1.4, 1.9, 2.4, 2.9, 3.4. All parameters except time step have been kept unmodified. This is a necessary operation in order to have the same number of steps per revolution. The optimization aims to figure out the TSR with the highest production of power. The simulation that has been previously analyzed, has been carried out with the optimized TSR at wind speed of 15 m/s obtained in the reference article [9]. With 10 m/s wind speed, the forces on the turbine are consequentially lower than at 15 m/s wind speed. It is likely the turbine will have to compensate this decrease by increasing TSR during the simulations. Curve might probably move a little rightward. This implies optimized TSR will be slightly higher. The resulting  $C_p$  for the considered TSRs are shown in Figure 11.

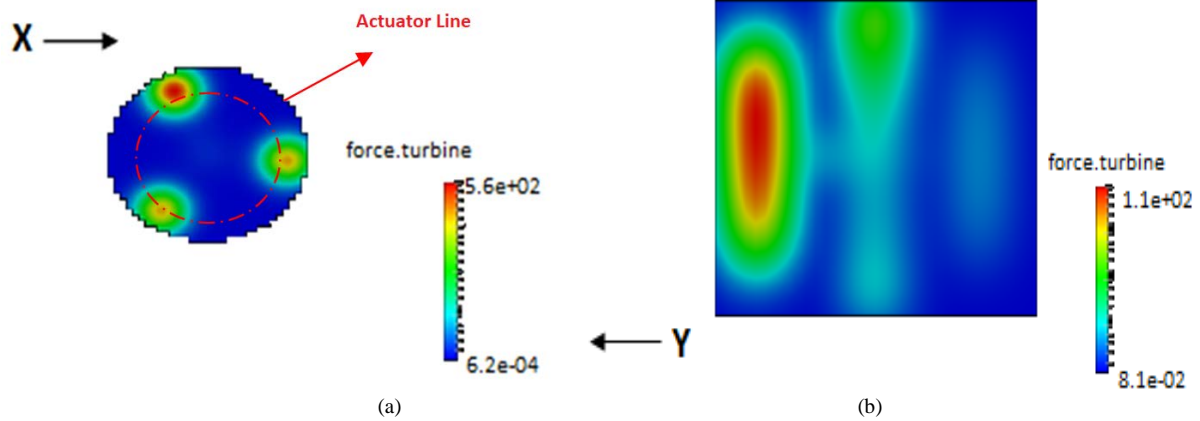


**Figure 10.** Force distribution (N m<sup>3</sup>/kg) (a) around the turbine in the x-y plane and (b) in the x-z plane

#### 4.3. Velocity profile

The model has been tested changing the free wind velocity, with 5 values from 5.5 m/s to 15 m/s. Theoretically, it is easy to predict that the higher the speed the higher the power. Power law should follow a cubic power trend. Since no electric production has been considered, no limit in power production has been taken into account. The resulting power as a function of wind speed is shown in Figure 12. The power follows the theoretical trend. Simulations demonstrated also that  $C_p$  increases a little when velocity increases. A higher speed implies a higher Reynolds number. Inertia forces prevail over the viscosity effects shaping a more uniform velocity field. This means higher lift and therefore the turbine works more efficiently.

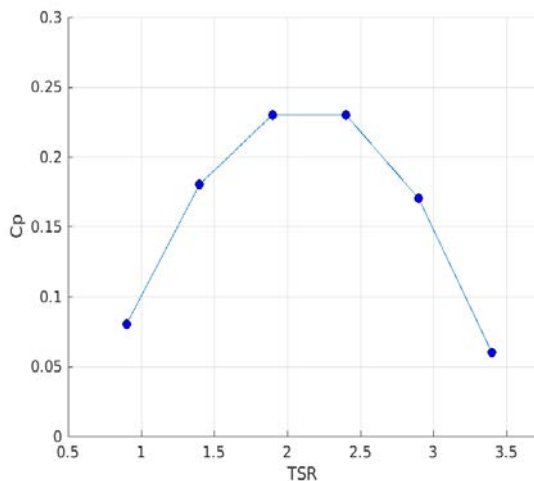


**Figure 11.** TSR change and  $C_p$

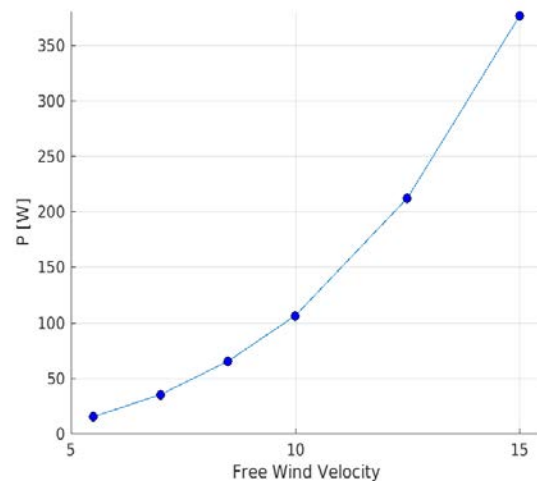


**Figure 12.** Velocity change and Power

#### 4.4. Study of different locations

For small scale wind turbine, power production may not be the only target. Very often the turbine is associated to the promotion of clean energy and to educational purposes [20]. Energy efficient locations need to be considered in relation to visibility. This is the case of the planned UiS project: research, education and promotion of clean energy are the main objectives and the power production itself has less importance. Two new locations have been tested. They have been named Position 2 and Position 3.

Locations have been chosen in the furthest part of the building with respect to the inlet and the fence, in order to have more uniform wind conditions. In addition, 1.5 m has been selected as distance from the nearest sides, considering this value acceptable to permit the turbine to be seen more easily. As Figure 13 indicates, these locations are closer to the east edge of the roof and, as consequence, easily spotted. Apart from the different position, all the other parameters and setting have been kept unmodified, i.e. the figure presents the flow conditions associated with the inlet wind velocity of 10 m/s from the west.

Compared to the previous position, which was selected according to wind study to maximize efficiency and power observing wind behavior and magnitude over the building, they present a less stable and uniform velocity field and a lower wind velocity. Especially for Position 3, power is expected to reduce dramatically. Wind speed at Position 2 does not change significantly with respect to Position 3, but Position 2 has a significantly lower efficiency, which brings to a reduction in produced power of 22%. Position 3 has a much lower wind speed, mainly due to the fence that the wind hits before flowing on the roof. This fence, creates low instabilities with which the efficiency becomes 0.13 and the power 25 W. Considering that Position 3 would be the overall most visible spot, UiS must take into consideration these results. Position 2 might be considered as a good trade-off between to fulfil the objectives of the project.

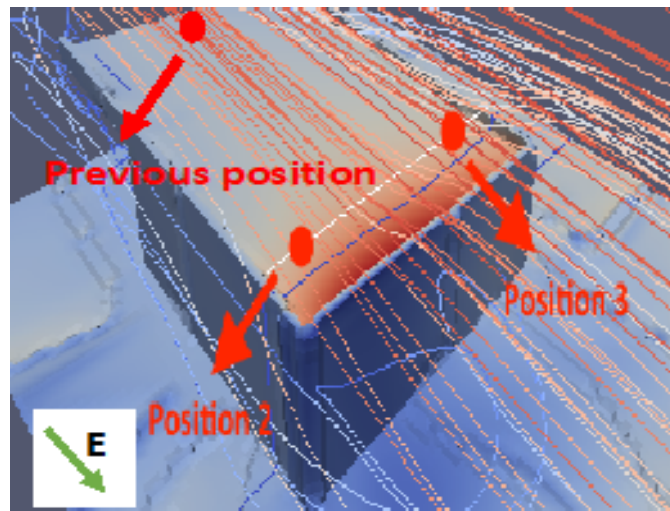


**Figure 13.** Position 2 and Position 3 locations

## 5. Conclusions

The aim of the study has been to create a flexible OpenFoam set up for investigation of wind flow over the campus buildings together with vertical axis wind turbine performance modeling. It should be possible to import different terrain model and campus model as well as different wind turbine representations based on the Actuator Line Model.

Built-environment wind turbines are growing in popularity. Nevertheless, examples of the implementation of this model for such type of turbines cannot be found. Therefore, starting from an OpenFOAM case involving laboratory setup, a new version of the model has been implemented. RANS  $k - \varepsilon$  has been chosen as turbulence model. Parameter studies were performed for TSR, wind velocity, turbine location and wind direction. Results appear to be coherent with the expectations. Power and power coefficient follow the theoretical outputs. As expected the model showed significant differences in power output depending on location and wind direction, which demonstrate the need for a thorough analysis before turbine installation.

## Acknowledgement

This research is based on a master thesis project involving the first author [5]. This study has been partially supported by Erasmus program funds.

## References

- [1] Government.no 2016 Renewable Energy  
<https://www.regjeringen.no/en/topics/energy/renewableenergy/id2000124/>
- [2] International Energy Agency 2016 Norway statistics  
<https://www.iea.org/statistics/statisticssearch/report/?country=NORWAY=&product=balances>
- [3] EWEA Business Intelligence 2015 *Aiming high: rewarding ambition in wind energy* (Brussels: The European Wind Energy Association)
- [4] Norwegian Wind Energy Association 2016 Wind power news <http://www.vindkraftnytt.no/>
- [5] Riva L 2017 *Implementation and application of the actuator line Model by OpenFOAM for a vertical axis wind turbine set on a University of Stavanger building roof* (Milan: Polytechnic of Milan)
- [6] Sørensen J N and Shen W Z 2002 Numerical modelling of wind turbine wakes *J. of Fluids Eng.* **124**(2) 393-399
- [7] Shamsoddin S and Porté-Agel F 2014 Large eddy simulation of vertical axis wind turbine wakes *Energies* **7**(2) 890-912
- [8] Schito P, Bernini L and Zasso A 2015 OpenFOAM for wind energy: wind turbine as a source term. Workshop HPC: methods for engineering. [https://hpc-forge.cineca.it/files/CoursesDev/public/2015/Workshop\\_HPC\\_Methods\\_for\\_Engineering/OpenFOAM\\_WindEnergy\\_schito.pdf](https://hpc-forge.cineca.it/files/CoursesDev/public/2015/Workshop_HPC_Methods_for_Engineering/OpenFOAM_WindEnergy_schito.pdf)
- [9] Bachant P, Goude A and Wosnik M 2016 Actuator line modeling of vertical-axis turbines *Wind Energy Rec.* **00** 1–17
- [10] Bachant P 2016 UNH-RVAT-3D-OpenFOAM <https://github.com/petebachant/UNH-RVAT-3D-OpenFOAM>
- [11] Bachant P, Goude A and Wosnik M 2016 turbinesFOAM  
<https://github.com/turbinesFoam/turbinesFoam>
- [12] Nuland S E 2017 *Wind Turbine Installation on offshore fish farm feed barge* (Stavanger: University of Stavanger)
- [13] Richards P J and Norris S E 2011 Appropriate boundary conditions for computational wind engineering models revisited *J. of Wind Eng. and Ind. Aerodynamics* **99** 257-266
- [14] Hargreaves D M and Wright N G 2007 On the use of the k-epsilon model in commercial CFD software to model the neutral atmospheric boundary layer *J. of Wind Eng. and Ind. Aerodynamics* **95** 355-369

- [15] Sheng W, Galbraith R A and Coton F N 2008 A modified dynamic stall model for low Mach numbers *J. of Solar Energy Eng.* **130(3)** 3-13.
- [16] Bachant P and Wosnik M 2016 Effects of Reynolds number on the energy conversion and near-wake dynamics of a high solidity vertical-axis cross-flow turbine *Energies* **9(2)** 73
- [17] Sheldahl R and Klimas P 1981 *Aerodynamic characteristics of seven symmetrical airfoil sections through 180-degree angle of attack for use in aerodynamic analysis of vertical axis wind turbines* (Albuquerque: Sandia National Laboratories)
- [18] CFD Direct 2016 The Architects of OpenFOAM. OpenFOAM USer Guide. <https://cfd.direct/openfoam/user-guide/>
- [19] Baldassarra G 2015 *Multidimensional CFD Simulation of a H-type Darrieus Vertical-Axis Wind Turbine with OpenFOAM* (Milan: Polytechnic of Milan)
- [20] Fields J, Oteri F, Preus R and Baring-Gould I 2016 *Deployment of Wind Turbines in the Built Environment: Risks, Lessons, and Recommended Practices* NREL (Golden: National Renewable Energy Laboratory).